

The use of strain sensors in an experimental modal analysis of small and light structures with free-free boundary conditions

Domen Rovšček¹, Janko Slavič¹ and Miha Boltežar¹

¹Laboratory for Dynamics of Machines and Structures, Faculty of Mechanical Engineering, University of Ljubljana, Aškerčeva 6, 1000 Ljubljana, Slovenia-EU.

Cite as:

D. Rovšček, J. Slavič and M. Boltežar

The use of strain sensors in an experimental modal analysis of small and light structures with free-free boundary conditions.

Journal of Vibration and Control, 2013, Volume 19, Issue 7, May 2013, Pages 1072-1079.

DOI: 10.1177/1077546312445058

Abstract

Small and light structures have distinctive features, which cause difficulties in the measurement of their modal parameters. The major issues are the mass, which is added to the measured structure by sensors, and the very high resonant frequencies. Those difficulties occur with a measurement of the excitation force. An innovative procedure for the experimental modal analysis of small and light structures was developed in this study. This procedure involves a measurement of the excitation force, which was performed by a piezo strain gauge that enables an analysis of the aforementioned structures with free-free support. The main advantage of this sensor in comparison to other devices used for force measurements is that it adds a very small mass to the measured structure (≈ 0.4 gram) but at the same time enables an accurate measurement of the modal parameters in a wide frequency range (up to 20 kHz). This makes it suitable for a measurement of the frequency-response functions of light structures that have high resonant frequencies. Consequently, an experimental modal analysis can be performed. The presented approach was experimentally tested on a sample with small dimensions and mass. The results of the experiment (modal parameters) were compared with the results of the numerical model. The good agreement between the results indicates that this procedure can be used on other similar structures.

Keywords

Experimental modal analysis, strain sensor, force measurement, high frequency, small structures, light structures

1 Introduction

Experimental Modal Analysis (EMA) is a procedure used to define the modal parameters (resonant frequencies, mode shapes and damping) of structures. It is thoroughly described in many publications [2, 7, 11, 14]. To perform an EMA the Frequency Response Functions (FRFs) at different points of the structure need to be measured. The measurement of the excitation force and the structure response (displacement, velocity or acceleration) have to be measured simultaneously to define the FRFs. The modal parameters can also be extracted only from the response measurement, without any information about the excitation force, but in this case there are difficulties with the correct scaling of the mode shapes, as Brincker and Andersen [3] have summarised. The extraction of the mode shapes from the response data only is known as Operational Modal Analysis (OMA) [20].

When larger structures are analysed there are no difficulties with achieving good results. In this case, an impact hammer or an (electro-magnetic) shaker is normally used for the excitation [7, 9, 14] and the force is transferred to the structure through a force sensor. But problems occur with relatively small and light structures (mass < 50 gram). The main reason is the mass added to the structure by the transducers (force sensor, accelerometer), which changes the structure's modal characteristics. Among others, this effect was researched by Huber *et al.* [12], Ozdoganlar *et al.* [15] and Silva *et al.* [16]. To avoid this problem, the response with no added mass can be measured with the use of non-contact sensors - most commonly the Laser Doppler Vibrometer (LDV) [12, 15, 18, 19]. But problems remain with the excitation force measurement, especially if results with a free-free support are required.

Some authors [12, 15, 18, 19] are describing methods for EMA on very small (micro) structures, but in these cases the structures are clamped on larger supporting bases and not freely supported. There are two possibilities to measure in this way. The first one is to excite a larger base with an ordinary (electro-magnetic) shaker and measure the response of the smaller structure, considering that the clamping of the structure to the base has influence on the results. This approach was described by Ozdoganlar *et al.* [15]. The second possibility is to fix a smaller structure to the base in one position and excite it with a non-contact device in another position. The non-contact excitation can be achieved by: a magnetostrictive actuator that excites a small ferromagnetic target fastened to the structure (Wilson and Bogy [19]), the interference of ultrasound frequencies in air (Huber *et al.* [12]), pressurised air (Vanlanduit *et al.* [18], Farshidi *et al.* [8]) and magnetostriction of the structure itself (Chakraborty *et al.* [6])

etc. Attaching masses to the structure changes the dynamical response and the free-free boundary conditions are still not possible.

In contrast to other methods the one used in this study enables the measurement of small and light structures with free-free support. The main advantages of this method are, that there is a relatively small attached mass to the structure and that torque transfer between the shaker and the measured structure is negligible. These properties make EMA on freely supported structures and a comparison between measurements and model results possible and easy to perform. The sensors that are used in this procedure allow measurements at relatively high frequencies (up to 20 kHz), which is suitable for small structures, because they usually have higher resonant frequencies [15].

A numerical model was built simultaneously with the measurement. The building of the model is straightforward, because the material and geometrical characteristics of the measured structure are well-known. The results of the model are relatively accurate, since the structure is quite simple and consists of only one piece of material without joints or other sources of nonlinearity [4, 5].

This study is organized as follows. Section 2 presents the theoretical aspects of this paper. Section 3 explains the use of the piezo strain gauge for the EMA. Section 4 presents the experiment and a comparison with the results of the numerical model. A summary of the work is given in Section 5.

2 Theoretical aspects

EMA is a procedure that is used to define the modal parameters of a structure. It is described in detail in [7, 11, 14]. The basic idea of the EMA is presented in Figure 1. The measured structure is excited with a known force $F_i(t)$ and the response $x_i(t)$ is measured simultaneously at the i -th measuring point. There are two ways to define the FRFs for all the measuring points. Either the excitation point is changed through all the positions and the response is measured always at the same point or the response measurement point is changed through all the positions and the excitation is always at the same point. The second possibility is used in this study, because it is harder to move the excitation point than the response measurement point. The measured time-domain signals $F_i(t)$ and $x_i(t)$ are then transformed into the frequency domain $F_i(\omega)$ and $X_i(\omega)$. The resonant frequencies are on the peaks of the FRFs ($H_i(\omega)$). The mode shapes and damping [17] are defined from the amplitudes and phases at these peaks. There are many methods for the extraction of modal parameters, one very simple one was presented by Maia and Ewins [13]. The geometrical characteristics of the structure and the locations of the response measurement points also need to be taken into consideration when extracting the mode shapes.

There are many methods that are used to assure the quality of the measured mode shapes. In this study the Modal Assurance Criterion (MAC), which is thoroughly described in many publications [1, 7, 14], was used. The MAC can be used for a validation of the experimental modal models or to calculate a correlation with the results of the numerical models. In the first case we talk

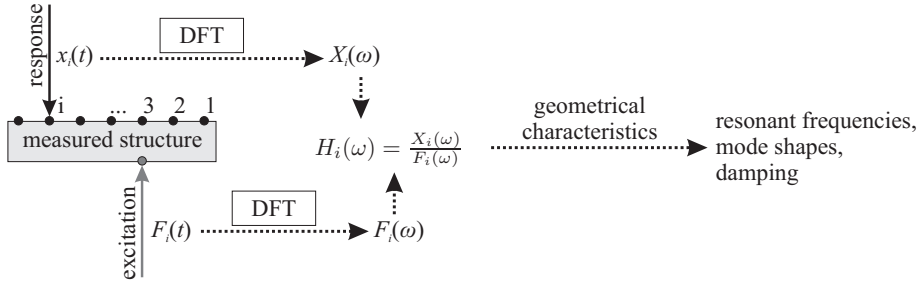


Figure 1: Illustration of the basic idea of EMA.

about Auto-MAC [10]. Auto-MAC was employed in this study to determine the quality of the experimental modal model, so the measured mode shapes were only compared to each other. The result of this procedure is a matrix with real values from 0 to 1. If the value that belongs to a pair of modes is equal to or close to 1, the modes are well correlated. When the modes are not in correlation, this value is close to 0. Due to the orthogonality the mode shapes are theoretically correlated only to themselves and not to the other modes. So the diagonal values of the Auto-MAC matrix should be close to 1 and non-diagonal values should be close to 0.

To describe the mode shapes modal vectors $\{\psi\}$ are used. Equation (1) gives the definition of Auto-MAC (AMAC) for j -th $\{\psi_X\}_j$ and k -th experimental mode $\{\psi_X\}_k$. Symbol * in Equation (1) denotes the complex conjugate.

$$AMAC \left(\{\psi_X\}_j, \{\psi_X\}_k \right) = \frac{\left| \{\psi_X\}_j^T \{\psi_X^*\}_k \right|^2}{\left(\{\psi_X\}_j^T \{\psi_X^*\}_j \right) \left(\{\psi_X\}_k^T \{\psi_X^*\}_k \right)} \quad (1)$$

3 The use of a piezo strain gauge for EMA

Measurements of FRFs were required to define the modal characteristics of the structure. During this measurement the excitation force and the response (velocity) of the structure were monitored simultaneously. When analysing larger structures the excitation is supplied through a force sensor and the response measured with an accelerometer. However, these two instruments affect the results when measuring smaller structures, because of the added mass. For this reason a Laser Doppler Vibrometer Polytec PDV-100 was used to measure the response and not to add any mass to the structure. The main question was, how to enable proper excitation. The goal was to measure the excitation force at

high frequencies as well as to define the modal parameters of the structure with as little external influence as possible. Consequently, a custom-made sensor was developed to measure the excitation force that was transferred from the shaker to the structure. The sensor is shown in Figure 2 and described in detail in Sections 3.1 and 3.2. An LDS V-101 electromagnetic shaker was used for the excitation. Its resonant frequency is at 12 kHz, which is inside the frequency range of the measurement. The results are not affected by the resonant frequencies of the shaker because the excitation force was measured and the influence of the shaker dynamics was therefore excluded from the measurements.

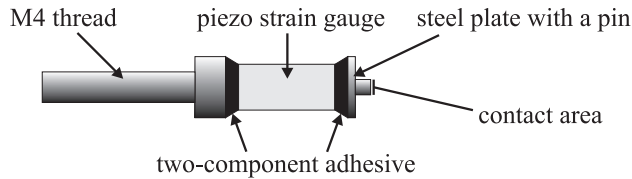


Figure 2: Schematic view of the sensor that was used to define the excitation force based on the measurement of strain.

3.1 Measurement of the excitation force

The sensor that was developed within this study is based on a piezo strain gauge (PCB 740B02) that has a relatively small mass (0.5 gram) and a high resonant frequency (100 kHz) in the direction of the measurement. This type of measuring device is usually fastened to a surface and then the strain of this surface is measured. But in this study the strain of the gauge itself is measured. This strain is caused by the excitation force that is transferred through the gauge. The measurement was set up this way, because the mass added to the structure is, in this case, smaller and the results are more accurate. The custom-made sensor consists of a piezo strain gauge and two elements that were fastened to it with a two-component adhesive (HBM X60). These two elements are an M4 thread that enables the sensor to be fixed to the shaker and a steel plate with a pin that is in contact with the measured structure. So as not to influence the FRFs, the pin has a small contact area (diameter 2.5 mm) with the measured structure, which allows only a minimal moment transfer from the shaker to the structure and vice versa. And also the design of the whole sensor makes it more flexible for bending and stiff in the longitudinal direction. The two-component adhesive used for fastening these parts together is based on Methyl Methacrylate and the manufacturer states it is made especially for bonding strain gauges to the measured surfaces. The adhesive is relatively stiff ($E \approx 13000 \text{ N/mm}^2$) when it reaches the hard state and is therefore suitable for high frequencies. These characteristics assure reliable measurements in the required frequency range (up to 20 kHz).

The force measurement was performed indirectly, because the sensor that was used is designed primarily to measure strain and not force. To execute the desired measurements it was first necessary to identify its sensitivity as a force sensor. The strain of the gauge ε_{sg} and the excitation force F_e are directly proportional, on the assumption that only the longitudinal force (compressive or tensile) is transferred through the sensor. The relation between ε_{sg} and F_e is defined by the conversion coefficient k_c , as shown in Equation (2).

$$k_c = \frac{F_e}{\varepsilon_{sg}} \quad (2)$$

The conversion coefficient of the sensor k_c , which transforms the measured strain into force, can be calculated by taking the strain ε_{sg} at a known load F_e . This known load is assured by first fixing an accelerometer (or other object with defined acceleration) with a known mass m_a on the sensor, as shown in Figure 3.

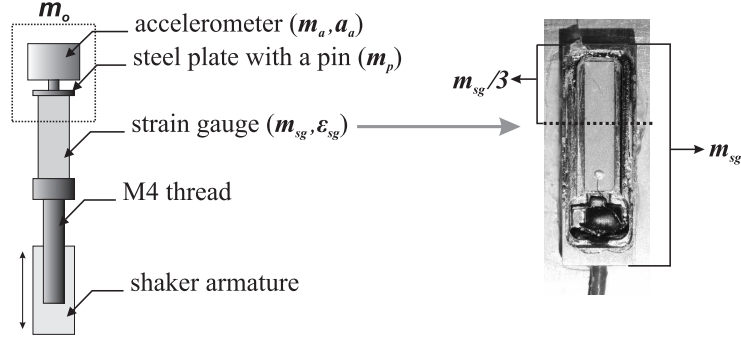


Figure 3: The calculation of the conversion coefficient k_c , taking into consideration the whole oscillating mass m_o .

In this case a simultaneous measurement of the strain of the gauge ε_{sg} and the acceleration of the accelerometer a_a is performed. When the whole oscillating mass m_o and its acceleration a_a are known, the excitation force ($F_e = m_o \cdot a_a$) is also known. Where the oscillating mass is used to denote the mass that exposes the dynamical force on the strain sensor; besides the mass of the accelerometer m_a and the steel plate with a pin m_p , also the mass of the glue and part of the strain sensor need to be considered. The glue was found to be lighter than 0.1 gram and therefore neglected. From the Figure 3 it can be seen, that the piezo crystal is located to the side of the strain-gauge and therefore as an estimate the one third of the strain-gauge mass was considered as the oscillating mass: $m_{sg}/3$ (0.5/3 gram). The total oscillating mass therefore is: ($m_o = m_a + m_p + m_{sg}/3$).

The entire calculation of k_c with the known excitation force F_e is described by Equation (3), which is derived from Equation (2). The calculated k_c represents

the conversion coefficient to transform the measured strain into an excitation force.

$$F_e = m_o \cdot a_a = \left(m_a + m_p + \frac{m_{sg}}{3}\right) \cdot a_a \quad \implies \quad k_c = \frac{\left(m_a + m_p + \frac{m_{sg}}{3}\right) \cdot a_a}{\varepsilon_{sg}} \quad (3)$$

This calculation was made with three different masses m_a ($m_{a,1} = 4.3$ gram, $m_{a,2} = 2.4$ gram and $m_{a,3} = 26$ gram). The mass of the adhesive and the mass of the strain-gauge are just a small part of the whole oscillating mass m_o . So even if their value is only roughly estimated, that does not affect the calculation of k_c significantly. For instance, a change of m_o for 0.1 gram (which means a relatively large difference of the mass of strain-gauge or adhesive) would only change k_c for 0.4 % when using $m_{a,3}$. The procedure for the mass $m_{a,3}$ is described in detail in Section 3.2.

The entire mass that is added to the structure during the measurement of FRFs equals $m_p + m_{sg}/3$, and it amounts to 0.4 gram. The mass that is usually added to the structure by commercially available force sensors is larger than 1 gram. This makes the device developed in this study more suitable for measurements on small and light structures.

3.2 Linearity of the force sensor

Three individual measurements with three different masses m_a were made to calculate the conversion coefficient k_c . A transfer function between the excitation force and the acceleration of the accelerometer was calculated to assure the linearity of the force sensor in the frequency range of the measurement. If the sensor functions correctly, then the ratio between the acceleration of the oscillating mass a_a and the excitation force F_e should remain the same throughout the whole frequency range, as shown in Equation (3). The linearity of the sensor was first tested with a PCB 357B40 accelerometer with mass $m_{a,1}$ and then with a Brüel & Kjær 4393 accelerometer with mass $m_{a,2}$. The third test was performed with a known mass $m_{a,3}$, as shown in Figure 4. The response of the mass was measured by LDV. The amplitude of the sensor's transfer function (the ratio between the measured a_a and ε_{sg} , which is proportional to F_e) vs. frequency can be seen in Figure 5. The correct functioning of the sensor is assured from 500 Hz to 20000 Hz.

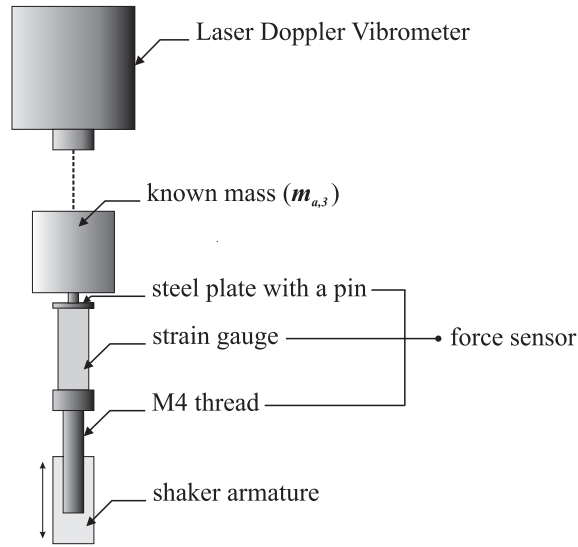


Figure 4: Measurement of the transfer function of the force sensor.

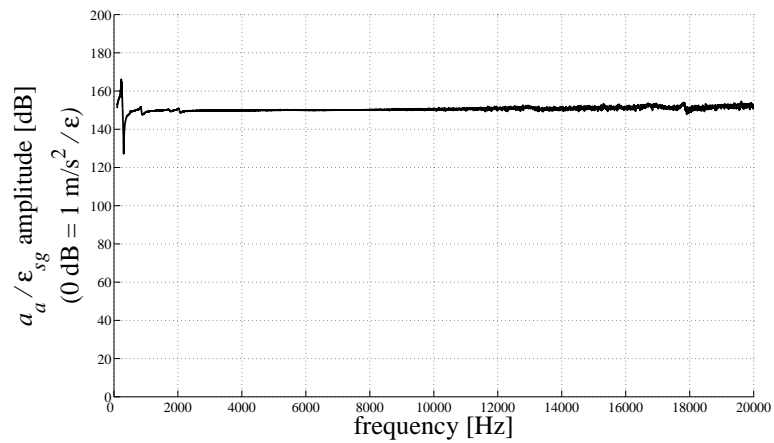


Figure 5: Amplitude of the sensor's transfer function (a_a/ϵ_{sg}) vs. frequency.

4 Experiment and comparison with the results of the numerical model

To test the quality of the force sensor, an EMA was performed on a sample with small dimensions and mass. The sample is a simple steel stick, so the

numerical model was built easily with commercial software using the Finite-Element Method (FEM). The measured modal parameters were compared with the numerical model results and validated with Auto-MAC.

4.1 Sample

A steel stick of circular cross-section with 6-mm diameter, 108-mm length and 21-gram mass was used for the sample, as shown in Figure 6. The geometry of the sample was chosen in such a way as to assure one axial, one torsional and many bending mode shapes in the frequency range of the measurement (0-20 kHz). The stick has a small, narrower section where the diameter is reduced to 1.4 mm (to lower the first axial resonant frequency) and two grooves (so that it is not axially symmetric).

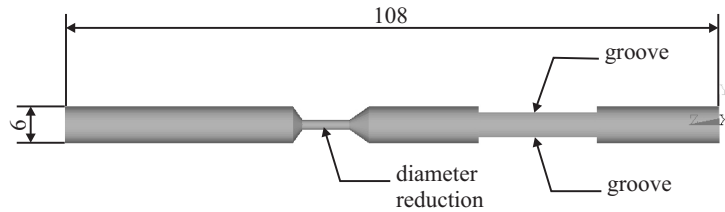


Figure 6: Sample that was used for the EMA.

4.2 FRF measurements

The sample was suspended with two strings to simulate the free-free support, as shown in Figure 7. The excitation was carried out in the horizontal direction with the use of a shaker that was also suspended with two strings. The measurement of the response was performed at fifteen points (1-15) in the X and Y directions and at two points (0, 16) in the Z direction. The measurement points are shown in Figure 8.

4.3 Comparison of the results of the experiment and the numerical model

The measured FRFs were used to calculate the modal parameters of the structure. To validate these modal parameters, a numerical model was built and compared with the results of the experiment. The sample that was used in the experiment had well-known material characteristics and geometry. Based on this, a relatively accurate FEM model was formed. The modal analysis was performed on the model and the results are calculated resonant frequencies and mode shapes. Viscous damping with constant damping ratio of 3 % was also

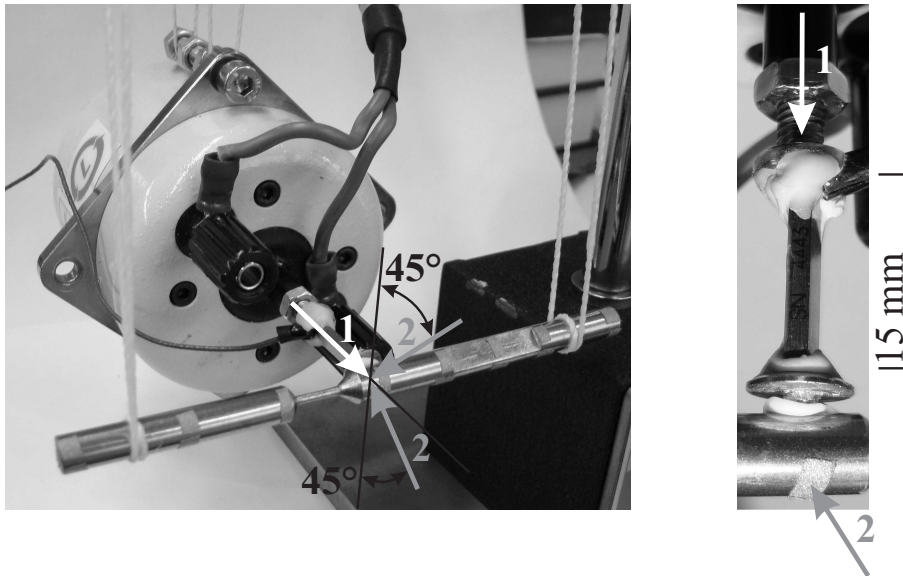


Figure 7: Measurement of the FRF: arrows marked with the number 1 indicate the excitation direction, arrows marked with the number 2 indicate the direction of the response measurement (left). Enlarged image of the contact region (right).

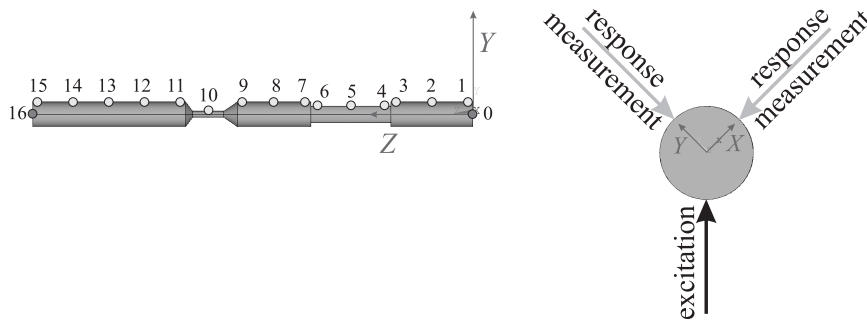


Figure 8: Measurement points for measurements in the direction of the Y axis (left). Excitation and response measurement direction (right).

introduced into the model, taking into account the measurement results. The comparison of the mode shapes obtained from the measurements and from the numerical model is shown in Figure 9. The difference between the results of the model and the measurements is, in most cases, lower than 2 % and in all cases lower than 4 %. Torsional mode shape (denoted by *) cannot be reconstructed

from the performed measurements, but it was possible to determine the corresponding resonant frequency (2279 Hz). All the other bending and axial mode shapes and the corresponding resonant frequencies were measured following the procedure that is described in Section 3. The resonant frequencies were also measured with an unknown impact excitation (with a steel impact ball), where only the response of the structure with no added mass was monitored by the LDV. The results showed that individual resonant frequencies with and without the added mass differ for less than 1.5 % (in majority of cases even less than 0.5 %), so the mass added to the structure is considered to have a negligible effect on the results.

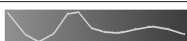
Numerical model			Measurement	
1	383 Hz			379 Hz
2	384 Hz			384 Hz
*	2268 Hz		/	2279 Hz
3	3551 Hz			3538 Hz
4	3938 Hz			3979 Hz
5	6902 Hz			6795 Hz
6	8415 Hz			8513 Hz
7	12390 Hz			12458 Hz
8	16979 Hz			17058 Hz
9	17679 Hz			18120 Hz
10	18269 Hz			18612 Hz
11	20196 Hz		> 20000 Hz	

Figure 9: Comparison of the numerical model and the measurement results. (* denotes the torsional mode shape, which cannot be reconstructed and was excluded from the Auto-MAC analysis)

To validate the measured mode shapes, they were compared with each other using Auto-MAC. The results are shown in Figure 10. As expected, the bending mode shapes that are in the frequency range of the sensor's correct functioning (500 Hz to 20000 Hz) are correlated with themselves but not with each other, so the diagonal Auto-MAC values are close to 1, and the non-diagonal values are close to 0. The axial mode shape (12521 Hz) also shows a small degree of correlation with the mode shape at 8513 Hz. This occurs because only a transversal

excitation was performed and there was no excitation in the axial direction. This could be improved if another measurement was performed with the excitation and response only in the axial direction. The first two mode shapes are below 500 Hz, which is the lower limit of the sensor's frequency range, and they are also very close together. This is why it is very difficult to distinguish between them. Consequently, the Auto-MAC values that describe the correlation between these two modes are very high (close to 1), which indicates that this is only a single mode shape. But if the response of the structure is examined, we can clearly distinguish two mode shapes and the model also predicts this. In comparison to the other mode shapes, the first two can also show larger Auto-MAC values, because of the measurement noise, which occurs below 500 Hz. The torsional mode shape (2279 Hz) was excluded from the Auto-MAC analysis, because it cannot be reconstructed from the performed measurements.

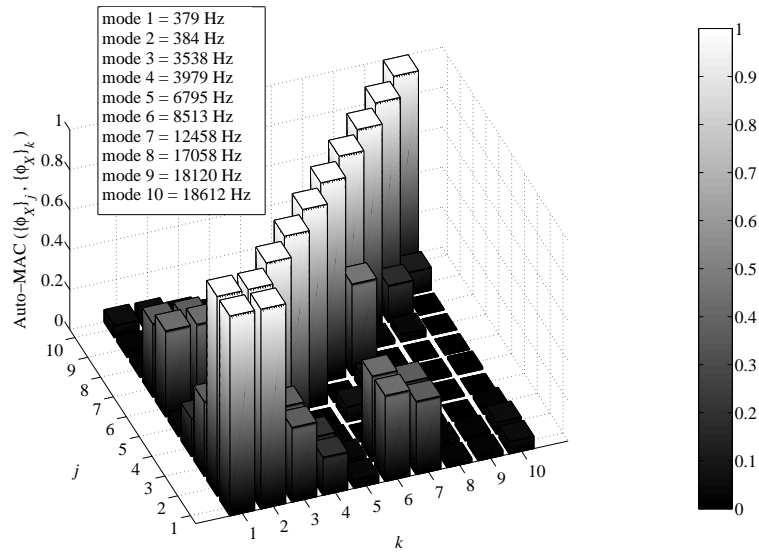


Figure 10: Correlation between the individual mode shapes using Auto-MAC.

5 Conclusion

An improved procedure for the experimental modal analysis of structures with relatively small dimensions and mass was presented. The structure is in contact with the excitation mechanism in this procedure. The measurement of the excitation force is performed with a piezo strain gauge, which was employed in a custom-made sensor. This kind of excitation force measurement can be used in a broad frequency range (up to 20 kHz), making it suitable for small structures that have higher resonant frequencies. At the same time, the mass added to the structure is minimal and has a negligible effect on the EMA.

The force sensor presented in this study was used for the EMA of a sample with small dimensions and mass. That analysis confirmed the correct functioning of the device. The EMA results were compared to numerical model results and it was found that they agree very well. The mode shapes are similar and the corresponding resonant frequencies are less than 4 % apart. In the range from 500 Hz to 20000 Hz the bending mode shapes are measured well.

The good agreement of the results indicates that the procedure described in this study can be used on other structures with similar characteristics (small dimensions and mass). The method is simple and assures accurate measurements of the FRFs, which are used to calculate the modal parameters of the structure. This procedure was tested on a homogenous structure that does not have any joints. Consequently, problems could occur with measurements of assembled structures, which show nonlinear contact and friction effects in the joints.

Acknowledgements

This research received no specific grant from any funding agency in the public, commercial, or not-for-profit sectors.

References

- [1] R. J. Allemang. The modal assurance criterion - Twenty years of use and abuse. *Sound and Vibration*, 37(8):14–23, 2003.
- [2] P. Avitabile. Experimental modal analysis: A simple non-mathematical presentation. *Sound and Vibration*, 35(1):20–31, 2001.
- [3] R. Brincker and P. Andersen. A Way of Getting Scaled Mode Shapes in Output Only Modal Testing. *Proceedings of IMAC-21: A Conference on Structural Dynamics*, pages 141–145, 2003.
- [4] D. Čelič and M. Boltežar. Identification of the dynamic properties of joints using frequencyresponse functions. *Journal of Sound and Vibration*, 317(1-2):158 – 174, 2008.

- [5] P. Čermelj and M. Boltežar. Modelling localised nonlinearities using the harmonic nonlinear super model. *Journal of Sound and Vibration*, 298(4-5):1099 – 1112, 2006.
- [6] S. Chakraborty, K. B. M. Swamy, S. Sen, and T. K. Bhattacharyya. An experimental analysis of electrostatically vibrated array of polysilicon cantilevers. *Microsystem technologies*, 16(12):2131–2145, 2010.
- [7] D. J. Ewins. *Modal Testing: Theory and Practice*. Research Studies Press, John Wiley and Sons, Lechworth, New York etc., 1984.
- [8] R. Farshidi, D. Trieu, S. S. Park, and T. Freiheit. Non-contact experimental modal analysis using air excitation and a microphone array. *Measurement*, 43(6):755–765, 2010.
- [9] J. A. Forrest. Experimental modal analysis of three small-scale vibration isolator models. *Journal of Sound and Vibration*, 289(1-2):382–412, 2006.
- [10] D. Fotsch and D. J. Ewins. Application of MAC in the Frequency Domain. *Proceedings of IMAC-18: A Conference on Structural Dynamics*, pages 1225–1231, 2000.
- [11] J. He and Z. F. Fu. *Modal Analysis*. Butterworth-Heinemann, Oxford, Boston etc., 2001.
- [12] T. M. Huber, M. Fatemi, R. Kinnick, and J. Greenleaf. Noncontact modal analysis of a pipe organ reed using airborne ultrasound stimulated vibrometry. *Journal of Acoustical Society of America*, 119(4):2476–2482, 2006.
- [13] N. M. M. Maia and D. J. Ewins. A new approach for the modal identification of lightly damped structures. *Mechanical Systems and Signal Processing*, 3(2):173–193, 1989.
- [14] N. M. M. Maia and J. M. M. Silva. *Theoretical and Experimental Modal Analysis*. Research Studies Press, John Wiley and Sons, Taunton, New York etc., 1997.
- [15] O. B. Ozdoganlar, B. D. Hansche, and T. Carne. Experimental modal analysis for microelectromechanical systems. *Experimental Mechanics*, 45(6):498–506, 2005.
- [16] J. M. M. Silva, N. M. M. Maia, and A. M. R. Ribeiro. Cancellation of mass-loading effects of transducers and evaluation of unmeasured frequency response functions. *Journal of Sound and Vibration*, 236(5):761–779, 2000.
- [17] J. Slavič and M. Boltežar. Damping identification with the morlet-wave. *Mechanical Systems and Signal Processing*, 25(5):1632 – 1645, 2011.
- [18] S. Vanlanduit, F. Daerden, and P. Guillaume. Experimental modal testing using pressurized air excitation. *Journal of Sound and Vibration*, 299(1-2):83–98, 2007.

- [19] C. J. Wilson and D. B. Bogy. An experimental modal analysis technique for miniature structures. *Journal of Vibration and Acoustics - Transactions of the ASME*, 118(1):1–9, 1996.
- [20] L. Zhang, R. Brincker, and P. Andersen. An Overview of Operational Modal Analysis: Major Development and Issues. *Proceedings of IOMAC-1*, pages 179–190, 2005.